Fabrication of Ion-enhanced Low-temperature tolerant graphene/PAA/KCl Hydrogel and its Application for Skin Sensors

Yaoyao Wang[a,b], *Longhang Zhu*[a,b], Haimei Lu[a,b], Xiangyu Kong[a], Chao Wang[a,*], Yong Huang[a], Min Wu[a,*]

[a]Technical Institute of Physics and Chemistry, Chinese Academy of Sciences, 29 Zhongguancun East Road, Haidian District, Beijing 100190, China.

[b]Center of Materials Science and Optoelectronics Engineering, University of the Chinese Academy of Sciences, 19 A Yuquan Rd, Shijingshan District, Beijing, 100049, China.

Corresponding Authors

[*]E-mail: wumin@mail.ipc.ac.cn (Min Wu)

[*]E-mail: chwangipc@mail.ipc.ac.cn (Chao Wang)

Tables & Figures

Table S1. The composition of GO_n/PAA-Fe_m hydrogels.

Hydrogels	GO (wt%)	$FeSO_4 \cdot 7H_2O$ (wt%)	H_2O_2 (mol%)	H_2SO_4 (mol%)	AA (wt%)	MBA (wt%)	Water (mL)
PAA	0	1	0.029	0.016	100	0.003	30
GO_n/PAA-Fe_1	0.3	1	0.029	0.016	100	0.003	30
	0.4	1	0.029	0.016	100	0.003	30
	0.5	1	0.029	0.016	100	0.003	30
	0.6	1	0.029	0.016	100	0.003	30
$GO_{0.5}$/PAA-Fe_m	0.5	0.00	0.029	0.016	100	0.003	30
	0.5	0.50	0.029	0.016	100	0.003	30
	0.5	0.75	0.029	0.016	100	0.003	30
	0.5	1.00	0.029	0.016	100	0.003	30
	0.5	1.25	0.029	0.016	100	0.003	30
	0.5	1.50	0.029	0.016	100	0.003	30

Notes: n presents the mass percentage of GO relative to acrylic acid, m presents the mass percentage of $FeSO_4 \cdot 7H_2O$ relative to acrylic acid.

Table S2. The volume of GO/PAA/KCl_{t-c} hydrogels.

Hydrogels	Diameter (mm)	Height (mm)	Volume (cm^3)
$GO_{0.5}$/PAA-Fe_1	57	5.28	13.47
GO/PAA/KCl_{12-5}	60	5.41	15.29
GO/PAA/KCl_{12-10}	58	5.35	14.13
GO/PAA/KCl_{12-15}	57	5.3	13.52
GO/PAA/KCl_{12-20}	55	4.83	11.47
GO/PAA/KCl_{4-20}	57	5.21	13.29
GO/PAA/KCl_{8-20}	56	5.02	12.36
GO/PAA/KCl_{16-20}	58	5.3	14.00

Table S3. The properties comparison with other anti-freezing hydrogels.

Stress (MPa)	Strain (%)	Ionic conductivity (S/m)	GF (at 25°C)	references
0.06	800	0.035 (25°C)	3.2	[1]
0.151	474	– –	– –	[2]
0.43	780	– –	2.69	[3]
0.17	4500	0.001 (25°C)	8.5	[4]
1.5	1769	– –	7.79	[5]
0.14	43	7.49 (25°C)	– –	[6]
0.168	1465	7.53 (-21°C)	– –	[7]
0.47	180	– –	– –	[8]
0.36	480	1 (25°C) 0.92 (-20°C)	2.84	[9]
0.0465	600	4.24 (25°C); 1.16 (-50°C)	2.173	[10]
0.37	1758	4.1 (-31.7°C)	1.744	[11]
2.65	1511	24.4 (25°C) 16.2 (-20°C)	8.66	*This study*

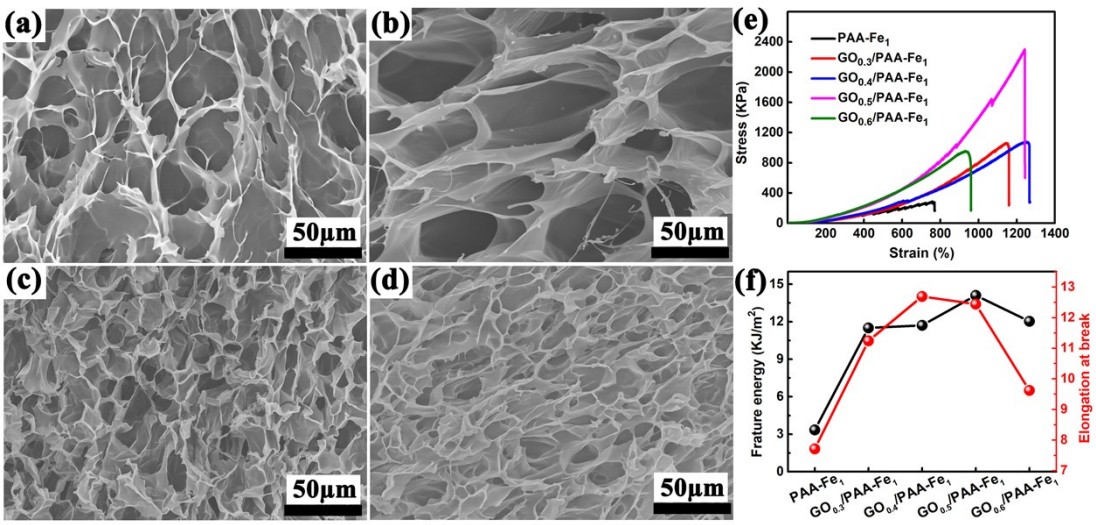

Figure S1. SEM images of GO_n/PAA-Fe_1 aerogels with different content of GO. (a) $GO_{0.3}$/PAA-Fe_1, (b) $GO_{0.4}$/PAA-Fe_1, (c) $GO_{0.5}$/PAA-Fe_1 and (d) $GO_{0.6}$/PAA-Fe_1 aerogels. The mechanical performance of GO_n/PAA-Fe_1 hydrogels. (e) Tensile stress-strain curves and (f) the fracture toughness and extension ratio under different content of GO.

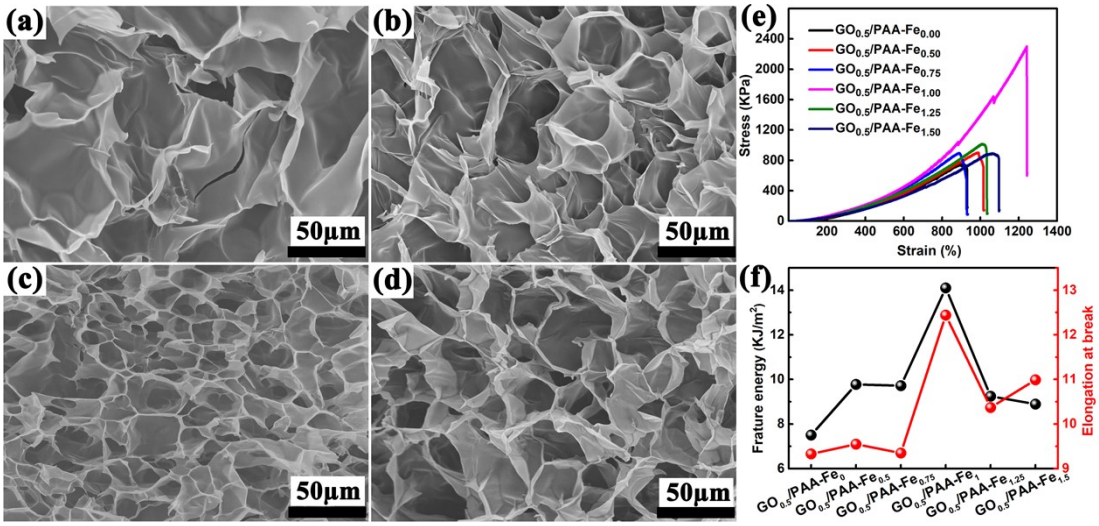

Figure S2. SEM images of $GO_{0.5}$/PAA-Fe_m aerogels with different content of $FeSO_4{\cdot}7H_2O$. (a) $GO_{0.5}$/PAA-$Fe_{0.5}$, (b) $GO_{0.5}$/PAA-$Fe_{0.75}$, (c) $GO_{0.5}$/PAA-$Fe_{1.25}$ and (d) $GO_{0.5}$/PAA-$Fe_{1.5}$ aerogels. The mechanical performance of $GO_{0.5}$/PAA-Fe_m hydrogels. (e) Tensile stress-strain curves and (f) the fracture toughness and extension ratio under different content of $FeSO_4 \cdot 7H_2O$.

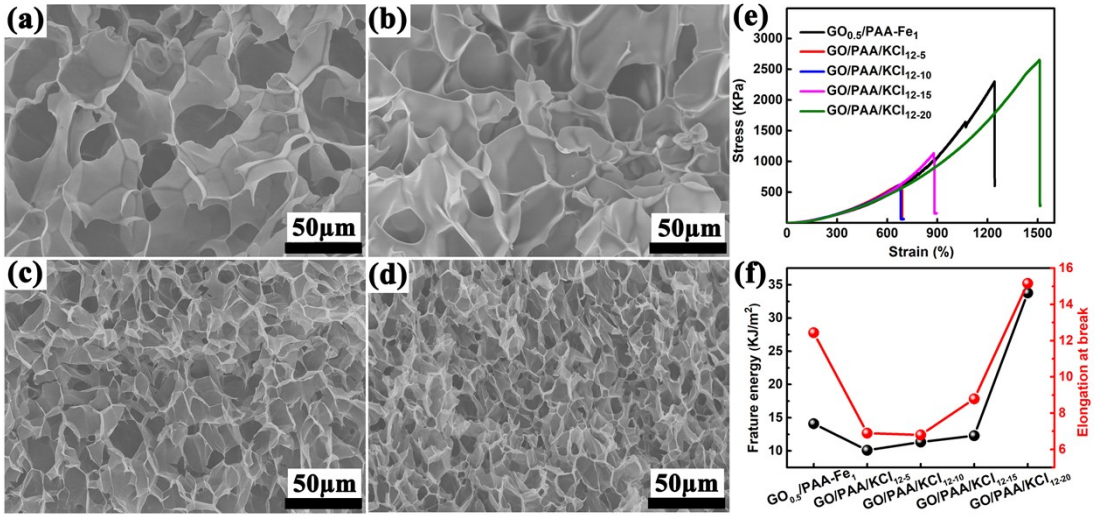

Figure S3. SEM images of GO/PAA/$KCl_{12\text{-}c}$ aerogels. (a) GO/PAA/$KCl_{12\text{-}5}$, (b) GO/PAA/$KCl_{12\text{-}10}$, (c)GO/PAA/$KCl_{12\text{-}15}$ and (d) GO/PAA/$KCl_{12\text{-}20}$ aerogels. (e) Tensile stress-strain curves and (f) the fracture toughness and extension ratio of various K^+-contained hydrogels .

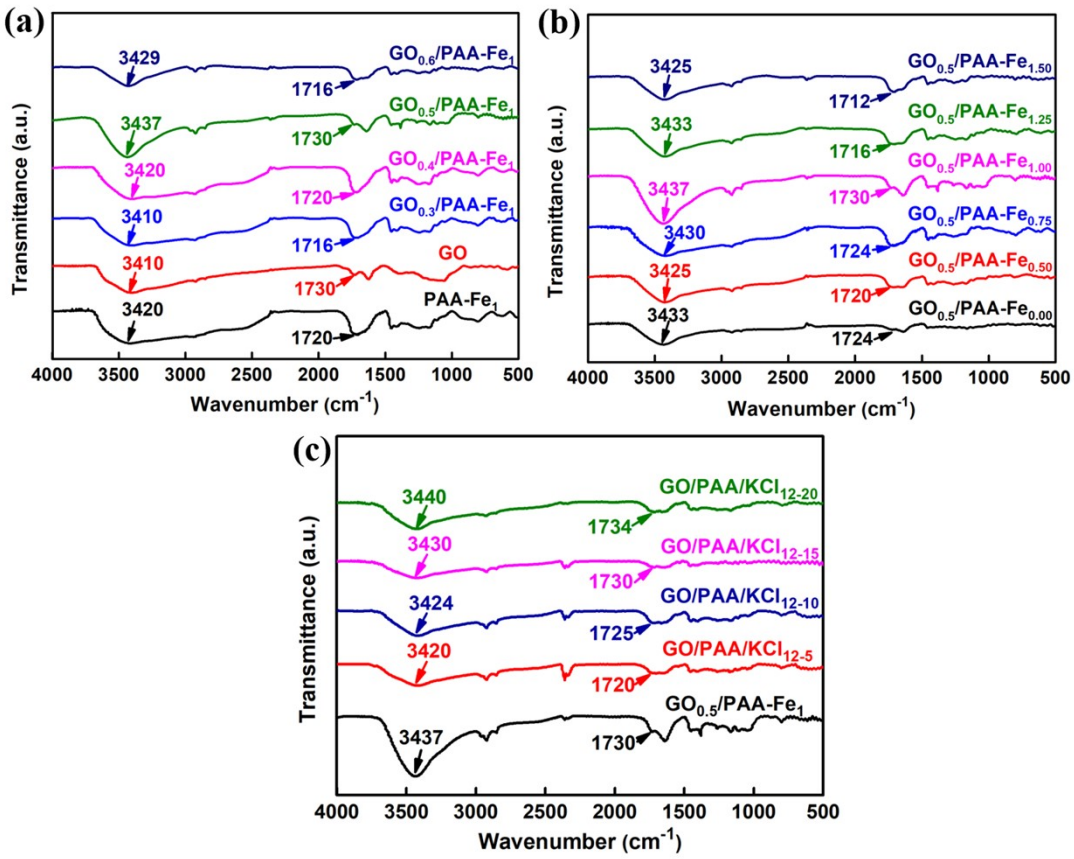

Figure S4. FT-IR spectra of GO_n/PAA-Fe_m and GO/PAA/KCl aerogels. (a) FT-IR spectra of GO_n/PAA-Fe_1 aerogels with different content of GO, (b) FT-IR spectra of $GO_{0.5}$/PAA-Fe_m aerogels with different content of $FeSO_4 \cdot 7H_2O$, (c) FT-IR spectra of GO/PAA/$KCl_{12\text{-}c}$ hydrogels.

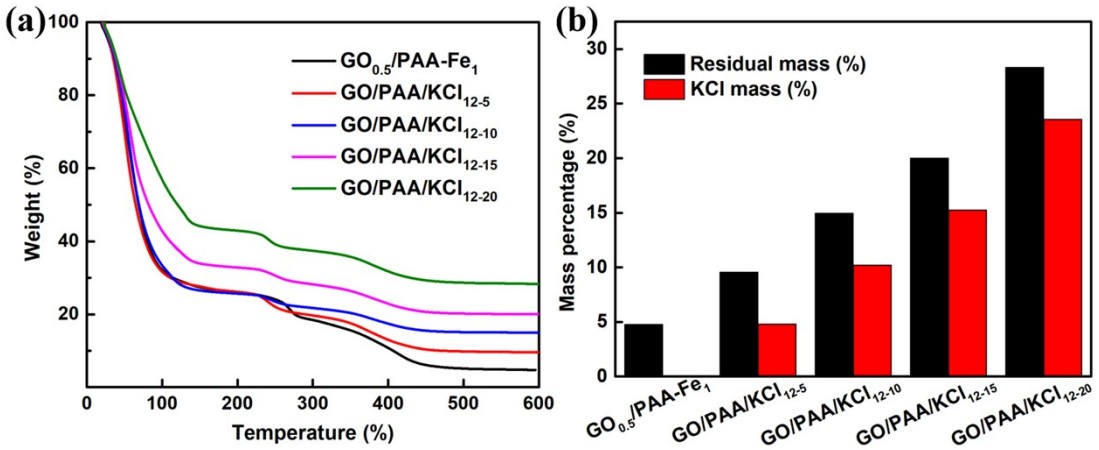

Figure S5. (a) The TGA curves and (b) the KCl content in GO/PAA/$KCl_{12\text{-}c}$ hydrogels.

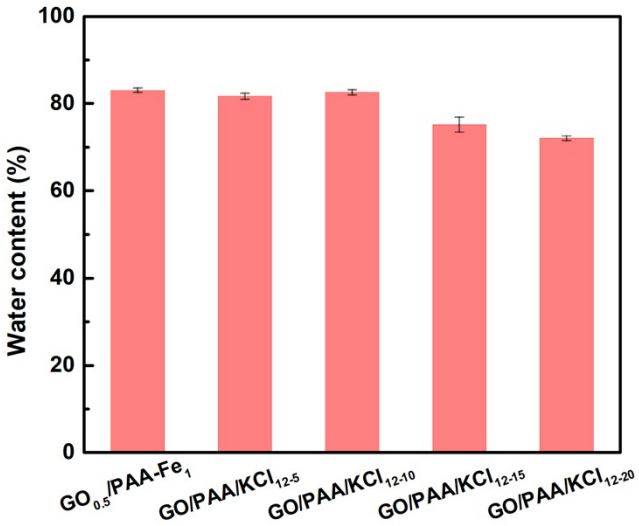

Figure S6. The water content of the GO/PAA/$KCl_{12\text{-}c}$ hydrogel.

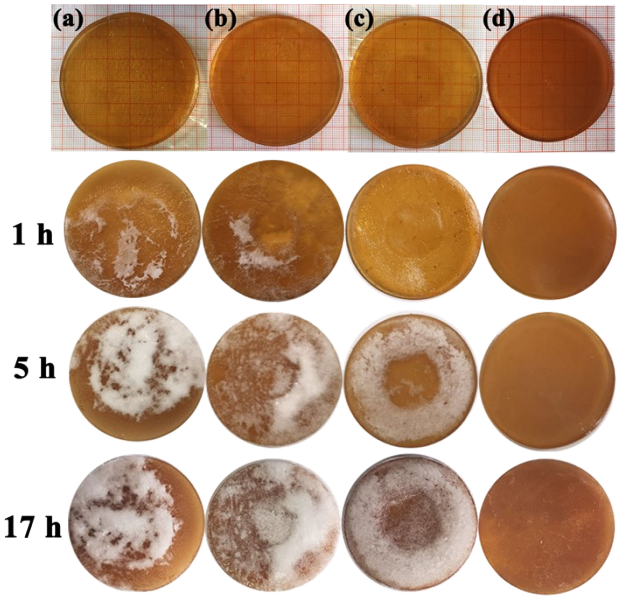

Figure S7. The appearance figures of hydrogels which soaked in different concentrations of KCl solutions for 12 h and then frozen at -20 °C for different times. (a) GO/PAA/$KCl_{12\text{-}5}$, (b) GO/PAA/$KCl_{12\text{-}10}$, (c) GO/PAA/$KCl_{12\text{-}15}$ and (d) GO/PAA/$KCl_{12\text{-}20}$ hydrogels.

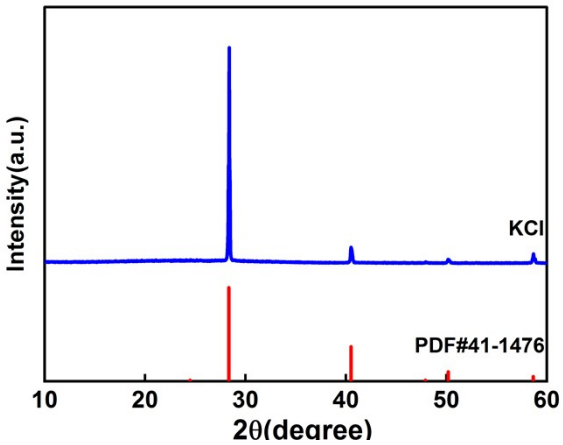

Figure S8. XRD patterns of KCl crystals isolated from the surface frost .

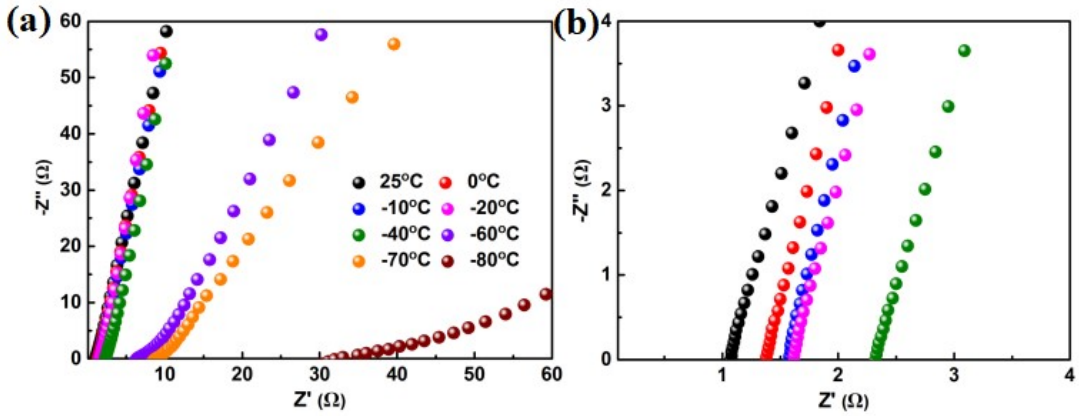

Figure S9. Electrochemical impedance spectroscopy (EIS) of GO/PAA/$KCl_{12\text{-}20}$ hydrogel at various temperatures. (b) is the magnification image of (a).

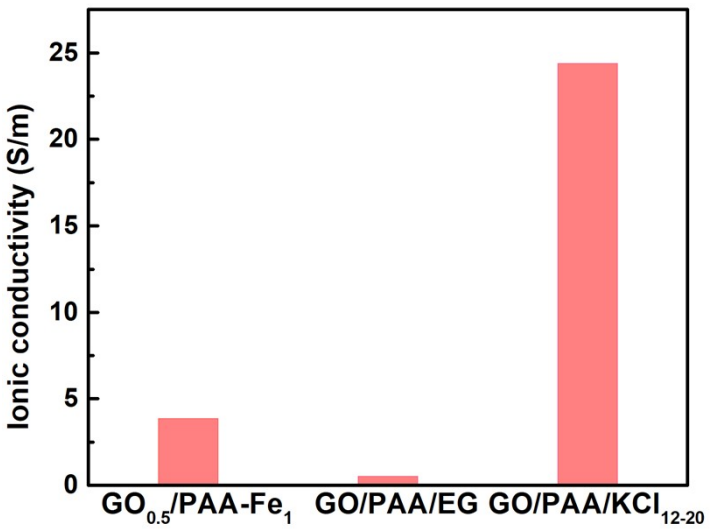

Figure S10. The ionic conductivity of various hydrogels at room temperature.

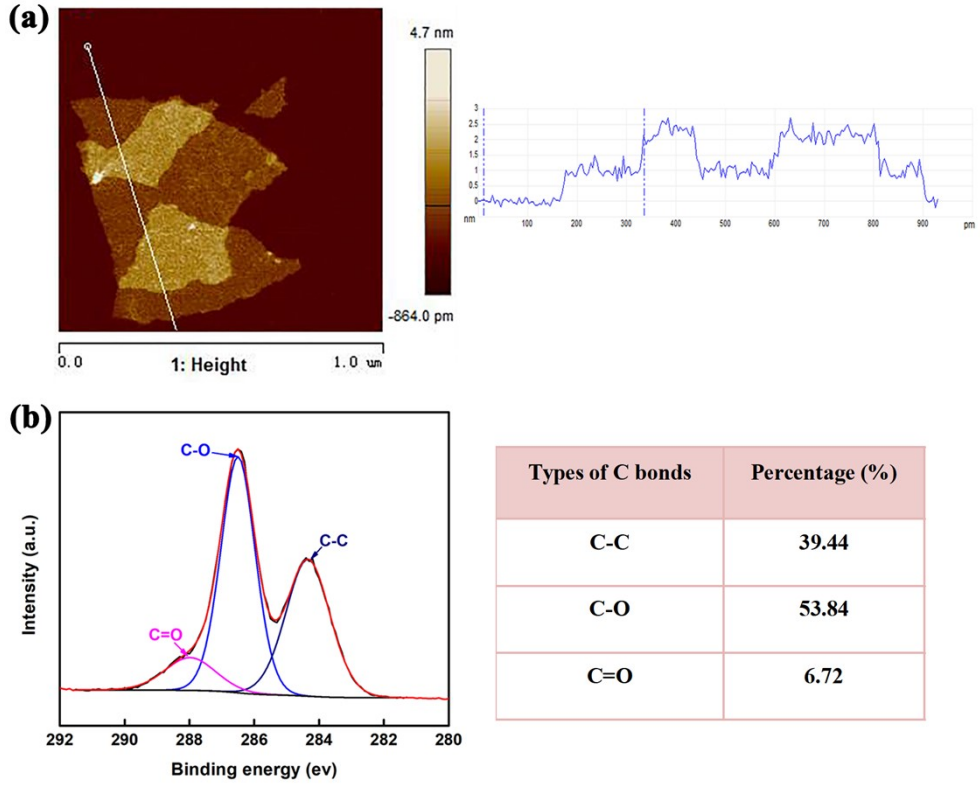

Types of C bonds	Percentage (%)
C-C	39.44
C-O	53.84
C=O	6.72

Figure S11. (a) The morphology characterization of GO by AFM. (b) XPS C1s spectra of GO and the percentage of different types C chemical bond.

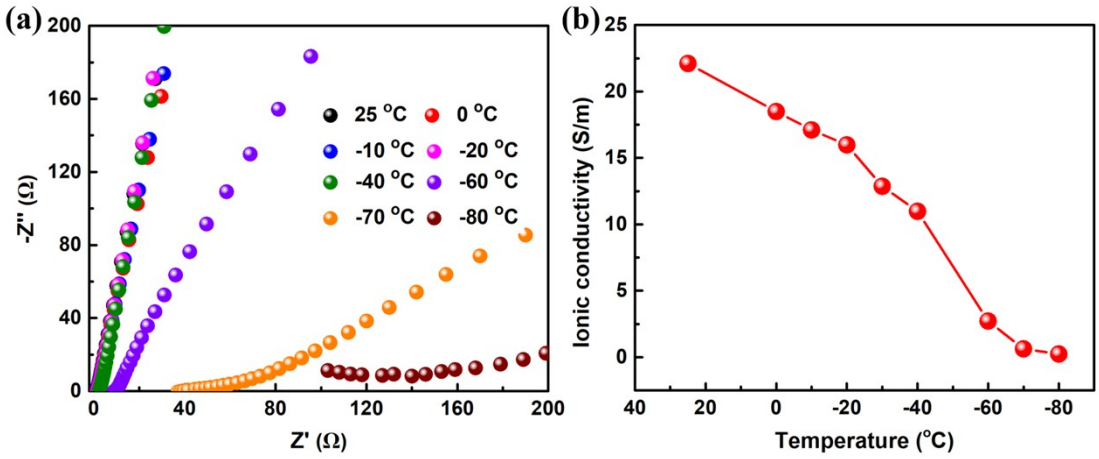

Figure S12. (a) Electrochemical impedance spectroscopy and (b) ionic conductivity of PAA/$KCl_{12\text{-}20}$ hydrogel at various temperatures.

References

[1] L. Wu, L. Li, M. Qu, H. Wang, Y. Bin, Mussel-Inspired Self-Adhesive, Antidrying, and Antifreezing Poly(acrylic acid)/Bentonite/Polydopamine Hybrid Glycerol-Hydrogel and the Sensing Application, ACS Applied Polymer Materials, 2 (2020) 3094-3106.

[2] Y.W. Shishan Xue, Meiling Guo, Yuanmeng Xia, Dan Liu, Hongwei Zhou and Weiwei Lei, Self-healable poly(acrylic acid-co-maleic acid)-glycerol-boron nitride nanosheet composite hydrogels at low temperature with enhanced mechanical properties and water retention, Soft Matter, 15 (2019) 3680-3688.

[3] X. Jing, P. Feng, Z. Chen, Z. Xie, H. Li, X.-F. Peng, H.-Y. Mi, Y. Liu, Highly Stretchable, Self-Healable, Freezing-Tolerant, and Transparent Polyacrylic Acid/Nanochitin Composite Hydrogel for Self-Powered Multifunctional Sensors, ACS Sustainable Chemistry & Engineering, 9 (2021) 9209-9220.

[4] H. Sun, Y. Zhao, S. Jiao, C. Wang, Y. Jia, K. Dai, G. Zheng, C. Liu, P. Wan, C. Shen, Environment Tolerant Conductive Nanocomposite Organohydrogels as Flexible Strain Sensors and Power Sources for Sustainable Electronics, Advanced Functional Materials, 31 (2021) 2101696.

[5] Q. Yu, Z. Qin, F. Ji, S. Chen, S. Luo, M. Yao, X. Wu, W. Liu, X. Sun, H. Zhang, Y. Zhao, F. Yao, J. Li, Low-temperature tolerant strain sensors based on triple crosslinked organohydrogels with ultrastretchability, Chemical Engineering Journal, 404 (2021) 126559.

[6] X.F. Zhang, X. Ma, T. Hou, K. Guo, J. Yin, Z. Wang, L. Shu, M. He, J. Yao, Inorganic Salts Induce Thermally Reversible and Anti-Freezing Cellulose Hydrogels, Angew Chem Int Ed Engl, 58 (2019) 7366-7370.

[7] L. Guan, S. Yan, X. Liu, X. Li, G. Gao, Wearable strain sensors based on casein-driven tough, adhesive and anti-freezing hydrogels for monitoring human-motion, J Mater Chem B, 7 (2019) 5230-5236.

[8] L.X. Wenhui Zheng, Yangyang Li, Yudong Huang, Bing Li, Zaixing Jiang, Guolin Gao, Anti-freezing, moisturizing, resilient and conductive organohydrogel for sensitive pressure sensors, Journal of Colloid and Interface Science, 594 (2021) 584-592.

[9] J. Wen, J. Tang, H. Ning, N. Hu, Y. Zhu, Y. Gong, C. Xu, Q. Zhao, X. Jiang, X. Hu, L. Lei, D. Wu, T. Huang, Multifunctional Ionic Skin with Sensing, UV-Filtering, Water-Retaining, and Anti-Freezing Capabilities, Advanced Functional Materials, 31 (2021) 2011176.

[10] T.Z. Chi Jiang, Huichao Liu, Guang Yang, Zhipeng He, Minjie Wang, Muwei Ji, Guangtao Cong, Jiali Yu, Caizhen Zhu and Jian Xu, A one-step aqueous route to prepare polyacrylonitrile-based hydrogels with excellent ionic conductivity and extreme low temperature tolerance, Journal of Materials Chemistry A, 8 (2020) 22090–22099.

[11] L.K.a.G.G. Xinyao Li, A bio-inspired self-recoverable polyampholyte hydrogel with low temperature sensing, Journal of Materials Chemistry B, 9 (2021) 2010- 2015.